JACS
JOURNAL OF THE AMERICAN CHEMICAL SOCIETY

COMMUNICATION

pubs.acs.org/JACS

Three-Dimensional Porous Metal−Metalloporphyrin Framework Consisting of Nanoscopic Polyhedral Cages

Xi-Sen Wang,[†] Le Meng,[†] Qigan Cheng,[†] Chungsik Kim,[†] Lukasz Wojtas,[†] Matthew Chrzanowski,[†] Yu-Sheng Chen,[‡] X. Peter Zhang,[†] and Shengqian Ma*[,†]

[†]Department of Chemistry, University of South Florida, 4202 East Fowler Avenue, Tampa, Florida 33620, United States

[‡]ChemMatCARS, Center for Advanced Radiation Sources, The University of Chicago, 9700 South Cass Avenue, Argonne, Illinois 60439, United States

Supporting Information

ABSTRACT: An unprecedented nanoscopic polyhedral cage-containing metal−metalloporphyrin framework, MMPF-1, has been constructed from a custom-designed porphyrin ligand, 5,15-bis(3,5-dicarboxyphenyl)porphine, that links Cu_2(carboxylate)$_4$ moieties. A high density of 16 open copper sites confined within a nanoscopic polyhedral cage has been achieved, and the packing of the porphyrin cages via an "ABAB" pattern affords MMPF-1 ultramicropores which render it selective toward adsorption of H_2 and O_2 over N_2, and CO_2 over CH_4.

Porphyrins and metalloporphyrins have, over the decades, been intensively studied for a range of applications.[1] The construction of metalloporphyrin-based nanoscopic polyhedral cages affords cage walls rich in π-electron density that can provide favorable interactions with targeted guests.[2] Such cages also contain multiple active metal centers that could facilitate synergistic interactions with substrates, as exemplified in metalloporphyrin supramolecular materials.[2−4] Concurrently, there has also been an escalating interest in constructing metalloporphyrin-based metal−organic framework (MOF) materials due to their potential applications for gas storage, sensors, and particularly heterogeneous catalysis.[5] It could be envisioned that, if the metalloporphyrin nanoscopic polyhedral cages are built into MOFs, then the π-electron-rich cage walls together with the high density of open metal sites within the confined nanospace would greatly benefit their gas storage and catalytic performances. Although a number of metalloporphyrin framework structures have been reported in the past decade,[5,6] polyhedral cage-type structures have not yet been incorporated into metalloporphyrin-based MOFs. Extensive efforts toward utilizing tetrakis(4-carboxyphenyl)porphyrin (tcpp) to assemble with highly symmetric secondary building units (SBUs) of 4- or 6-connectivity to target the polyhedral cage-type metalloporphyrin framework structure, have generally afforded 2D layered structures or 3D pillared structures in which the active metal centers within the porphyrin rings are usually blocked,[5c−e,6h−j] although some 3D channeled structures with accessible metal centers have been reported recently.[6d,g,k,l] This is likely an artifact of the symmetry of tcpp, which means that it plays the role of a node that is not suitable for the formation of polyhedral cages when connecting highly symmetric SBUs.[7] Therefore, the incorporation of polyhedral cages into metalloporphyrin-based MOFs remains a challenge and necessitates the custom design of new porphyrin ligands that will be more suited to serve as linkers. In this contribution, we report the first example of such a MOF, which is based upon a metal−organic polyhedron (MOP) formed from a custom-designed porphyrin ligand and a judiciously selected SBU. The MOP serves as a supermolecular building block (SBB) that sustains a 3D porous metalloporphyrin framework structure exhibiting a very high density of open metal sites in the confined nanoscopic polyhedral cage.

[M_2(carboxylate)$_4$] paddlewheel moieties have been widely used for the construction of MOPs as they are ubiquitous in coordination chemistry and their square geometry is versatile in this context.[8] In particular, vertex-linking of the square SBUs with isophthalate ligands allows the generation of various types of faceted MOPs.[9] The utilization of these faceted MOPs as SBBs has only recently been employed for the construction of highly porous and symmetrical MOFs by bridging the isophthalates with various organic moieties through their 5-positions, as well exemplified by MOPs based upon isophthalate derivatives and square dicopper paddlewheel SBUs.[9d,10] Encouraged by these systems, we anticipate incorporating the porphyrin moiety into a MOP by designing an isophthalate-derived porphyrin ligand, 5,15-bis(3,5-dicarboxyphenyl)porphine (bdcpp), in which a pair of isophthalates are bridged by a porphine macrocycle (Scheme 1a). The assembly of bdcpp with dicopper paddlewheel SBUs (Scheme 1b) afforded an unprecedented 3D porous metalloporphyrin framework, MMPF-1 (MMPF denotes Metal−MetalloPorphyrin Framework), consisting of nanoscopic polyhedral cages with 16 open copper sites.

MMPF-1 was obtained as dark red block crystals via solvothermal reaction of bdcpp and copper nitrate in dimethylacetamide (DMA) at 85 °C. Single-crystal X-ray crystallographic studies[11] conducted using synchrotron radiation at the Advanced Photon Source, Argonne National Laboratory, revealed that MMPF-1 crystallizes in the space group $I4/m$ and consists of dicopper paddlewheel SBUs linked by bdcpp ligands.

In the bdcpp ligand, the four carboxylate groups and the two phenyl rings of the isophthalate moieties are almost coplanar, whereas the dihedral angle between the porphyrin ring and the phenyl rings is 69.2°. Sixteen bdcpp ligands connect eight paddlewheel SBUs to form a nanoscopic cage. Four dicopper paddlewheel SBUs are bridged by four isophthalate moieties of

Received: May 11, 2011
Published: September 28, 2011

Scheme 1. (a) 5,15-Bis(3,5-dicarboxyphenyl)porphyrin (bdcpp) Ligand and (b) Dicopper Paddlewheel SBU

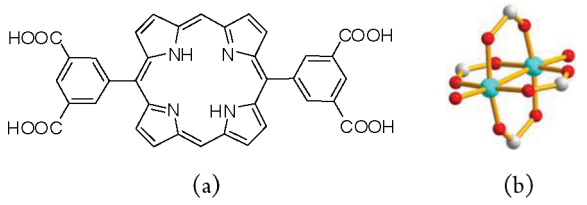

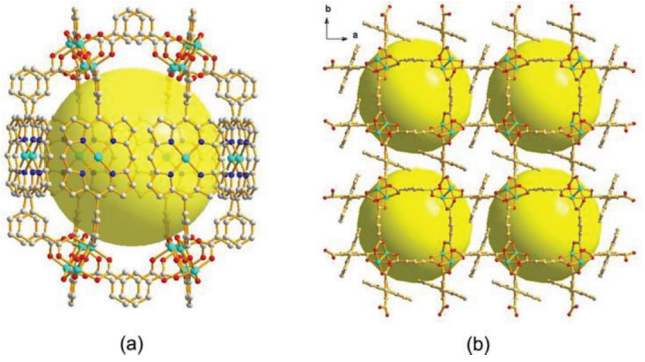

Figure 1. (a) Nanoscopic cage enclosed by eight dicopper paddlewheel SBUs and 16 bdcpp ligands (eight are face-on porphyrins, and the other eight only provide isophthalate units). (b) One layer of nanoscopic cages extended in the *ab* plane (hydrogen atoms omitted for clarity).

four different bdcpp ligands to form the top of the cage; they are pillared to four dicopper paddlewheel SBUs at the bottom of the cage through eight different bdcpp ligands (Figure 1a). The porphyrin macrocycle of the bdcpp ligand is metalated *in situ* by Cu(II) ion that is free of coordinated solvent molecules, probably due its unavailability for axial ligation,[6a] thus leaving both the distal and proximal positions open. The porphyrin ring of each bdcpp is in close contact with two adjacent porphyrin rings, one of which lies parallel (2.850 Å between an H atom of one porphyrin ring and the plane of the porphyrin ring of an adjacent bdcpp ligand), whereas the other lies orthogonal (2.554 Å between an H atom of one porphyrin ring and the plane of the adjacent porphyrin). The cage contains three types of window: there are two square windows formed by four dicopper paddlewheel SBUs through four isophthalate moieties with dimensions of 8.070 Å × 8.070 Å (atom-to-atom distance) (Figure S1a); there are eight rectangular windows formed by two dicopper paddlewheel SBUs and two half-porphyrin rings via three isophthalate motifs with dimensions of 7.065 Å × 7.181 Å (Figure S1b); there are eight triangular windows formed by linking one dicopper paddlewheel SBU with two half-porphyrin rings through two isophthalate motifs with dimensions of 6.979 Å × 6.979 Å × 7.640 Å (Figure S1c). In each cage, there are eight open copper sites associated with the porphyrin rings of the bdcpp ligands and eight open copper sites from dicopper paddlewheel SBUs that are activated by thermal liberation of aqua ligands. The distance between copper atoms within the opposite porphyrin rings is 18.615 Å, whereas copper atoms in adjacent porphyrin rings are separated by 7.571 and 7.908 Å; open copper sites from two opposite dicopper paddlewheel SBUs at the top and the bottom of the cage lie 16.170 Å apart,

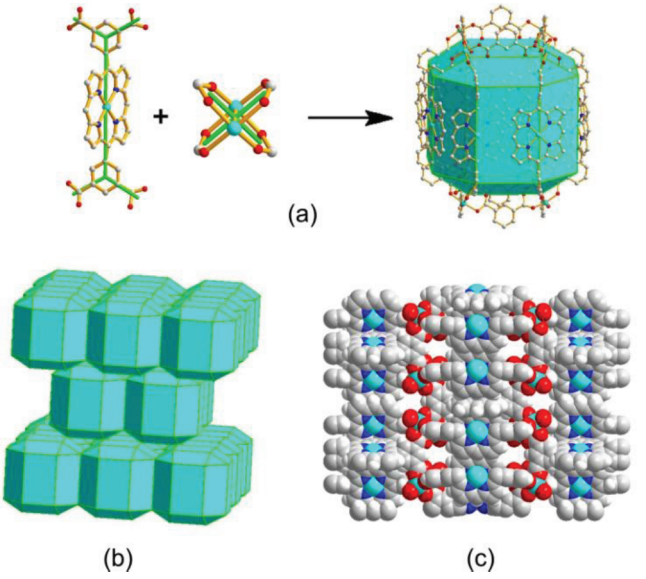

Figure 2. (a) Illustration of linking bdcpp ligand and dicopper paddlewheel to form the irregular rhombicuboctahedral cage. (b) "ABAB" packing of rhombicuboctahedron layers in MMPF-1. (c) Space-filling model on the [1 0 0] plane indicating the open pore size of ~3.4 Å × 3.5 Å.

whereas open copper sites from adjacent SBUs lie 8.070 Å apart. The volume of the cage is ~2340 Å^3, and it is filled with highly disordered solvent molecules of DMA and water that cannot be mapped by single-crystal X-ray studies, even using a synchrotron radiation source. All 16 open copper sites point toward the center of the cage, an unprecedentedly high density of open metal sites in a nanoscopic cage (~7 open metal sites/nm^3) (Figure 1a).

If one connects the centers of all isophthalate phenyl rings and the centers of the eight paddlewheels, the cage can be depicted as a polyhedron that has 24 vertices, 26 faces, and 48 edges (Figure 2a). In view of its similar shape to the rhombicuboctahedron connected by 24 isophthalates and 12 paddlewheels in MOPs and some MOFs,[9d,10b] this polyhedron can be also described as an irregular rhombicuboctahedron. These irregular rhombicuboctahedra serve as SBBs to extend in the *ab* plane (Figure 1b) and then pack along *c* via "ABAB" stacking to form an overall 3D structure (Figure 2b). Topologically, MMPF-1 can be described as a 3D 4-connected net possessing *lvt*-like topology (Figure S2).[12]

Due to the ABAB packing, the two square windows and eight triangular windows of each nanoscopic cage are totally blocked, whereas the eight rectangular windows are eclipsed with remaining apertures of ~3.4 Å × 3.5 Å (van der Waals distance), as can be viewed from the [1 0 0] (Figure 2c), [0 1 0] (Figure S3a), and [1 1 1] directions (Figure S3b). These tiny apertures could let very small molecules like water (kinetic diameter 2.64 Å) pass through but could hardly allow the DMA solvent molecules (molecule size ~5.24 Å × 4.52 Å × 4.35 Å) that are trapped in the irregular rhombicuboctahedral cages to escape.

Thermogravimetric analysis (TGA) of the fresh MMPF-1 sample (Figure S4) reveals that the first weight loss of 25.95% (calcd 25.33%) from 20 to ~170 °C corresponds to loss of two DMA molecules adsorbed on the surface, six H_2O guest molecules trapped in the irregular rhombicuboctahedral cages, and the two terminal aqua ligands liberated from the copper paddlewheel SBUs. A steady plateau from ~170 to ~240 °C is followed

dx.doi.org/10.1021/ja204339e |*J. Am. Chem. Soc.* 2011, 133, 16322–16325

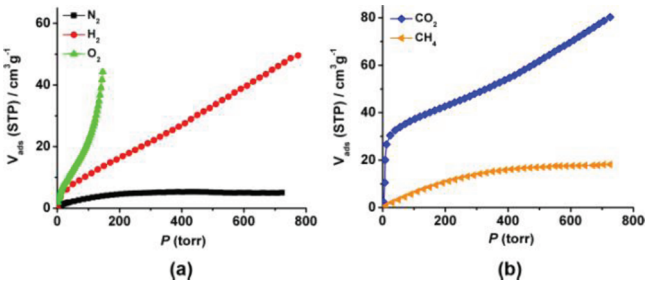

Figure 3. Gas adsorption isotherms of MMPF-1 at (a) 77 and (b) 195 K.

by the loss of two DMA guest molecules trapped in the cages (found 14.34%; calcd 13.32%), presumably accompanied by decomposition of the copper paddlewheel SBUs[13] at ~360 °C. The loss of bdcpp ligands starts from ~370 °C and finishes at ~450 °C, and results in complete collapse of the MMPF-1 framework.

The tiny pore sizes of MMPF-1, which are a result of the "ABAB" packing of the irregular rhombicuboctahedral cages, prompted us to evaluate its performance as a selective gas adsorbent. A freshly prepared MMPF-1 sample was washed with methanol and thermally activated at 120 °C under dynamic vacuum before gas adsorption measurements. N_2 adsorption isotherms were collected at 77 K, and as shown in Figure 3a, a very limited amount of N_2 (5 cm^3/g) is adsorbed on the external surface of MMPF-1 at ~760 Torr. In contrast, a larger amount of H_2 uptake (50 cm^3/g) is observed under the same condition, and a substantial uptake of 45 cm^3/g is also found for O_2 at its saturation pressure of 154 Torr at 77 K. Gas adsorption studies at 195 K indicated that MMPF-1 can uptake a large amount of CO_2 (80 cm^3/g) at 760 Torr, which is much higher than the amount of CH_4 (18 cm^3/g). The interesting molecular sieving effect observed for MMPF-1 can be attributed to its small aperture sizes of ~3.5 Å, which exclude larger gas molecules of N_2 and CH_4 with kinetic diameters of 3.64 and 3.8 Å, respectively, but allow the entry of smaller gas molecules of H_2 (kinetic diameter 2.89 Å), O_2 (kinetic diameter 3.46 Å), and CO_2 (kinetic diameter 3.3 Å). The selective adsorption of H_2 and O_2 over N_2, and CO_2 over CH_4, observed for MMPF-1 is rare;[14] to the best of our knowledge, it represents the first example reported in metalloporphyrin-based MOFs. Our attempts to remove the DMA guest molecules trapped in the nanoscopic cages by activating MMPF-1 at 200 °C in order to improve its uptake capacities of H_2 and CO_2 unfortunately led to partial collapse of the framework, as evidenced by a significant decrease of CO_2 uptake (Figure S5) and loss of crystallinity (Figure S6), which indicates its modest thermal stability.

In summary, by employing the SBB strategy, an unprecedented three-dimensional porous metal−metalloporphyrin framework that consists of nanoscopic rhombicuboctahedral cages with a high density of 16 open copper sites has been prepared, based upon the custom-designed bdcpp ligands that link copper paddlewheel SBUs. The "ABAB" packing of the rhombicuboctahedral cages in MMPF-1 constricts its pore size, which facilitates selective adsorption of H_2 and O_2 over N_2, and CO_2 over CH_4. Considering the high density of open metal sites confined within a nanoscopic cage, ongoing work in our laboratories will focus upon designing new porphyrin ligands to construct cage-containing porous metalloporphyrin frameworks with larger pore sizes, and to explore them for applications in gas storage, sensors, and particularly heterogeneous catalysis for small molecules.

■ ASSOCIATED CONTENT

Supporting Information. Experimental procedures for the syntheses of bdcpp ligand and MMPF-1, single-crystal X-ray diffraction experiment, structural pictures, PXRD patterns, TGA plot, and procedures for gas adsorption experiments, as well as the single-crystal X-ray diffraction data in CIF format. This material is available free of charge via the Internet at http://pubs.acs.org.

■ AUTHOR INFORMATION

Corresponding Author
sqma@usf.edu

■ ACKNOWLEDGMENT

The authors acknowledge the University of South Florida for financial support of this work. This work was also supported, in part, by the University of South Florida Internal Awards Program under Grant No.18325. The authors also thank Prof. Mike Zaworotko for helpful discussions. The crystal diffraction of MMPF-1 was carried out at the Advanced Photon Source on beamline 15ID-C of ChemMatCARS Sector 15, which is principally supported by the National Science Foundation/Department of Energy under grant number NSF/CHE-0822838. Use of the Advanced Photon Source was supported by the U.S. Department of Energy, Office of Science, Office of Basic Energy Sciences, under Contract No. DE-AC02-06CH11357.

■ REFERENCES

(1) Kadish, K. M.; Smith, K. M.; Guilard, R.; Eds. *The Porphyrin Handbook*; Academic Press: San Diego, 2000−2003.

(2) (a) Nakamura, Y.; Aratani, N.; Osuka, A. *Chem. Soc. Rev.* **2007**, *36*, 831–845. (b) Beletskaya, I.; Tyurin, V. S.; Tsivadze, A. Y.; Guilard, R.; Stern, C. *Chem. Rev.* **2009**, *109*, 1659–1713.

(3) Drain, C. M.; Varotto, A.; Radivojevic, I. *Chem. Rev.* **2009**, *109*, 1630–1658.

(4) (a) Song, J.; Aratani, N.; Shinokubo, H.; Osuka, A. *J. Am. Chem. Soc.* **2010**, *132*, 16356–16357. (b) Meng, W.; Breiner, B.; Rissanen, K.; Thoburn, J. D.; Clegg, J. K.; Nitschke, J. R. *Angew. Chem., Int. Ed.* **2011**, *50*, 3479–3483. (c) O'Sullivan, M. C.; Sprafke, J. K.; Kondratuk, D. V.; Rinfray, C.; Claridge, T. D. W.; Saywell, A.; Blunt, M. O.; O'Shea, J. N.; Beton, P. H.; Malfois, M.; Anderson, H. L. *Nature* **2011**, *469*, 72–75.

(5) (a) Kosal, M. E.; Suslick, K. S. *J. Solid State Chem.* **2000**, *152*, 87–98. (b) Suslick, K. S.; Bhyrappa, P.; Chou, J.-H.; Kosal, M. E.; Nakagaki, S.; Smithenry, D. W.; Wilson, S. R. *Acc. Chem. Res.* **2005**, *38*, 283–291. (c) Goldberg, I. *Chem. Commun.* **2005**, 1243–1254. (d) Goldberg, I. *CrystEngComm* **2008**, *10*, 637–645. (e) DeVries, L. D.; Choe, W. *J. Chem. Crystallogr.* **2009**, *39*, 229–240.

(6) (a) Abrahams, B. F.; Hoskins, B. F.; Michail, D. M.; Robson, R. *Nature* **1994**, *369*, 727–729. (b) Kumar, R. K.; Goldberg, I. *Angew. Chem., Int. Ed.* **1998**, *37*, 3027–3040. (c) Lin, K.-J. *Angew. Chem., Int. Ed.* **1999**, *38*, 2730–2732. (d) Kosal, M. E.; Chou, J.-H.; Wilson, S. R.; Suslick, K. S. *Nat. Mater.* **2002**, *1*, 118–121. (e) Smithenry, D. W.; Wilson, S. R.; Suslick, K. S. *Inorg. Chem.* **2003**, *42*, 7719–7721. (f) Ohmura, T.; Usuki, A.; Fukumori, K.; Ohta, T.; Ito, M.; Tatsumi, K. *Inorg. Chem.* **2006**, *45*, 7988–7990. (g) Shultz, A. M.; Farha, O. K.; Hupp, J. T.; Nguyen, S. T. *J. Am. Chem. Soc.* **2009**, *131*, 4204–4205. (h) Choi, E.-Y.; Wray, C. A.; Hu, C.; Choe, W. *CrystEngComm* **2009**, *11*, 553–555. (i) Choi, E.-Y.; Barron, P. M.; Novotny, R. W.; Son, H.-T.;

Hu, C.; Choe, W. *Inorg. Chem.* **2009**, *48*, 426–428. (j) Chung, H.; Barron, P. M.; Novotny, R. W.; Son, H.-T.; Hu, C.; Choe, W. *Cryst. Growth Des.* **2009**, *9*, 3327–3332. (k) Barron, P. M.; Wray, C. A.; Hu, C.; Guo, Z.; Choe, W. *Inorg. Chem.* **2010**, *49*, 10217–10219. (l) Farha, O. K.; Shultz, A. M.; Sarjeant, A. A.; Nguyen, S. T.; Hupp, J. T. *J. Am. Chem. Soc.* **2011**, *133*, 5652–5655.

(7) O'Keeffe, M. *Chem. Soc. Rev.* **2009**, *38*, 1215–1217.

(8) (a) Ni, Z.; O'Keeffe, M.; Yaghi, O. M. *Angew. Chem., Int. Ed.* **2008**, *47*, 5136–5147. (b) Li, J.-R.; Yakovenko, A.; Lu, W.; Timmons, D. J.; Zhuang, W.; Yuan, D.; Zhou, H.-C. *J. Am. Chem. Soc.* **2010**, *132*, 17599–17610. (c) Li, J.-R.; Zhou, H.-C. *Nature Chem.* **2010**, *2*, 893–898. (d) Li, J.-R.; Zhou, H.-C. *Angew. Chem., Int. Ed.* **2009**, *48*, 8465–8468.

(9) (a) Ke, Y.; Collins, D. J.; Zhou, H.-C. *Inorg. Chem.* **2005**, *44*, 4154–4156. (b) Furukawa, H.; Kim, J.; Plass, K. E.; Yaghi, O. M. *J. Am. Chem. Soc.* **2006**, *128*, 8398–8399. (c) Perry, J. J.; Kravtsov, V. C.; McManus, G. J.; Zaworotko, M. J. *J. Am. Chem. Soc.* **2007**, *129*, 1076–1077. (d) Perry, J. J.; Perman, J. A.; Zaworotko, M. J. *Chem. Soc. Rev.* **2009**, *38*, 1400–1417.

(10) (a) Nouar, F.; Eubank, J. F.; Bousquet, T.; Wojtas, L.; Zaworotko, M. J.; Eddaoudi, M. *J. Am. Chem. Soc.* **2008**, *130*, 1833–1835. (b) Cairns, A. J.; Perman, J. A.; Wojtas, L.; Kravtsov, V. C.; Alkordi, M. H.; Eddaoudi, M.; Zaworotko, M. J. *J. Am. Chem. Soc.* **2008**, *130*, 1560–1561.

(11) X-ray crystal data for MMPF-1: $C_{36}H_{16}Cu_3N_4O_{10}$, fw = 855.15, tetragonal, *I*4/*m*, *a* = 18.615(7) Å, *b* = 18.615(7) Å, *c* = 36.321(1) Å, *V* = 12586(9) Å^3, *Z* = 8, *T* = 100 K, ρ_{calcd} = 0.903 g/cm^3, R_1 ($I > 2\sigma(I)$) = 0.0960, wR_2 (all data) = 0.2042.

(12) Perman, J. A.; Cairns, A. J.; Wojtas, L.; Eddaoudi, M.; Zaworotko, M. J. *CrystEngComm* **2011**, *13*, 3130–3133.

(13) (a) Chui, S. S.-Y.; Lo, S. M.-F.; Charmant, J. P. H.; Orpen, A. G.; Williams, I. D. A. *Science* **1999**, *283*, 1148–1150. (b) Schlichte, K.; Kratzke, T.; Kaskel, S. *Microporous Mesoporous Mater.* **2004**, *73*, 81–88. (c) Yuan, D.; Zhao, D.; Timmons, D. J.; Zhou, H.-C. *Chem. Sci.* **2011**, *2*, 103–106.

(14) (a) Dybtsev, D. N.; Chun, H.; Yoon, S. H.; Kim, D.; Kim, K. *J. Am. Chem. Soc.* **2004**, *126*, 32–33. (b) Chen, B.; Ma, S.; Zapata, F.; Fronczek, F. R.; Lobkovsky, E. B.; Zhou, H.-C. *Inorg. Chem.* **2007**, *46*, 1233–1236. (c) Ma, S.; Wang, X.-S.; Collier, C. D.; Manis, E. S.; Zhou, H.-C. *Inorg. Chem.* **2007**, *46*, 8499–8501. (d) Ma, S.; Wang, X.-S.; Yuan, D.; Zhou, H.-C. *Angew. Chem., Int. Ed.* **2008**, *47*, 4130–4133. (e) Ma, S. *Pure Appl. Chem.* **2009**, *81*, 2235–2251. (f) Li, J.-R.; Kuppler, R. J.; Zhou, H.-C. *Chem. Soc. Rev.* **2009**, *38*, 1477–1504.